JOURNAL OF APPLIED ELECTROCHEMISTRY 24 (1994) 1001–1008

A study of the delay effect in $SOCl_2$ batteries

M. KOVAČ, M. GABERŠČEK, S. PEJOVNIK

National Institute of Chemistry, PO Box 30, Ljubljana, Slovenia

Received 30 July 1993; revised 6 December 1994

Electrical and microstructural properties of the passive layers formed on lithium in $SOCl_2$ containing different additives (PVC, inorganic salts, cathode additives) were studied. LiCl crystals were found to be cubic, octahedral or needle-like. Typical passive layer thicknesses were 1–20 μm. The electrical properties of the passive layer were explained by referring to the space charge model of SEI conduction. It was pointed out that impedance spectroscopy may be selectively used as a non-destructive method for estimation of the galvanostatic behaviour of lithium batteries. The best results, as regards the elimination of the delay effect, were obtained with a combination of organic and inorganic electrolyte additives.

1. Introduction

When lithium is exposed to liquid $SOCl_2$ a solid passive layer, consisting mostly of LiCl, is formed on its surface. The passive layer properties have been studied by many authors using various techniques: scanning electron microscopy [1,2] combined with EDS analysis [1], impedance spectroscopy [2,3], calorimetry [4], potentiostatic and galvanostatic pulse techniques [5–7]. It has been commonly accepted that the passive layer acts as a solid electrolyte interphase (SEI). Furthermore, the fact that the layer is a much better ionic than electronic conductor allows this system to be used as a battery.

However, as regards the precise mechanism of the electric conduction across the passive layer, many questions have remained open. For example, it is known that certain electrolyte additives essentially modify the morphology and the thickness of the passive layer and, on the other hand, reduce the so-called delay effect (i.e. the initial voltage or current drop on a step excitation [6–8,15,16,21,22]. The reason for this and whether there is a relationship between the morphology of the passive layer, its thickness and the delay effect phenomena, remains unclear. Another question which is crucial to the electrical properties of the Li/passive layer/electrolyte system concerns the porosity of the passive layer. Two extreme views have been expressed: (a) pores containing liquid electrolyte cover almost the entire passive layer [9] and (b) less than 50% of the passive layer volume contains open pores [1]. However, the role of polycrystallinity and doping in the layer's conductivity has hardly been discussed.

The most comprehensive picture of processes occurring on passivated lithium anodes under various conditions has been given by Peled [10], Fig. 1(a). His classical SEI model is based on the assumption that electrical transport across the passivated lithium is determined by the bulk migration of lithium vacancies through a thin compact part of the passive layer. The actual thickness of the compact part is a function of many variables: storage time, overpotential, temperature, electrolyte additives etc. To explain unpredictable results of certain measurements (e.g. the delay effect, etc.) special processes, such as mechanical cracking of the layer or layer dissolution and reprecipitation were involved.

Recently, we have shown that a different, but still consistent, picture of the passive layer behaviour is obtained if it is assumed that the principal barrier to the electrical transport in the Li/passive layer/$SOCl_2$ system is associated with the Li/passive layer interface, rather than with the bulk of the passive layer itself [11]. In the present paper the experimental results are explained, mainly by referring to this, the so-called space-charge model, which is an analogy of the Schottky diode in solid state ionics, Fig. 1(b).

The main purpose of the present investigation was to prepare Li/$SOCl_2$ batteries with a reduced delay effect by using appropriate electrolyte and cathode additives and to explain the mechanism(s) of this reduction. The effect of additives on the passive layer microstructural features was studies by scanning electron microscopy/energy dispersive spectroscopy (SEM/EDS) while the electrical behaviour of the passivated lithium anodes was investigated by impedance spectroscopy and the galvanostatic pulse technique.

2. Experimental details

Lithium, as well as the electrolyte and cathode components, reacts vigorously with moisture. Preparation of test cells was carried out in the dry room facility of Weiss Technik. The relative humidity was kept below 1% in the dry room.

Four different types of $SOCl_2$ electrolyte were prepared: 1.5 M $LiAlCl_4/SOCl_2$ (further designated as A), 1.5 M $LiAlCl_4/SOCl_2 + 2\,g\,dm^{-3}$ PVC (designated as B), 1.5 M $LiAlCl_4/SOCl_2 + 0.034$ M $LiAl(SO_3Cl)_4 + 0.6$ M SO_2 (designated as C) and 1.5 M $LiAlCl_4/SOCl_2 + 0.034$ M $LiAl(SO_3Cl)_4 + 0.6$ M $SO_2 + 2\,g\,dm^{-3}$ PVC (designated as D). Electrolyte A was prepared

0021-891X © 1994 Chapman & Hall

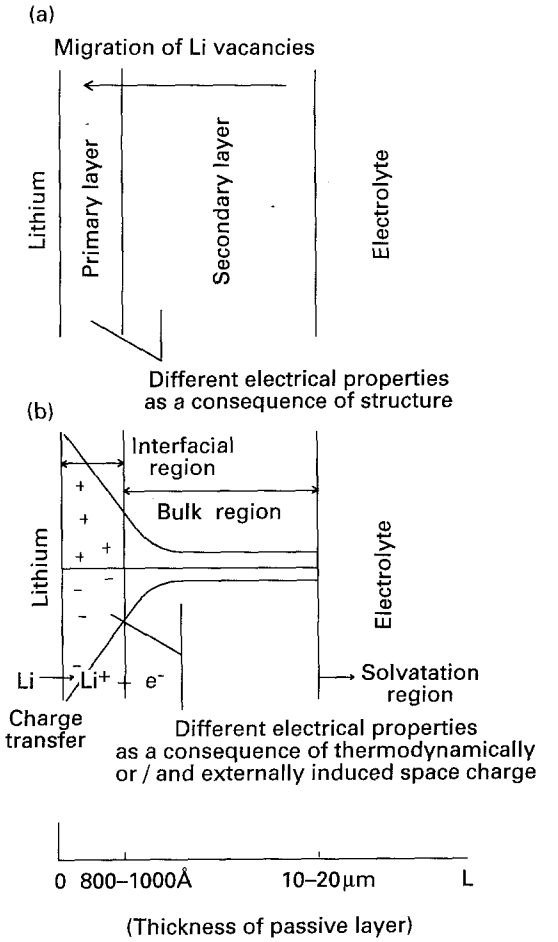

Fig. 1. Comparison between (a) the classical (SEI) model and (b) the space charge model of the $Li/SOCl_2$ passive layer.

by mixing equimolar amounts of LiCl and $AlCl_3$ into pure $SOCl_2$ (Fluka). Electrolyte A served as the reference electrolyte to which the other electrolytes were compared.

Type B was the solution of electrolyte A in which chlorinated polymer (PVC, Solvic) was dissolved. Type C was a weakly acidic catholyte with the addition of inorganic salt of chlorosulphonic acid and SO_2. It was prepared by known amounts of $AlCl_3$ p.a., Li_2CO_3 p.a. and LiCl p.a., dissolved in freshly distilled $SOCl_2$ (Fluka). The addition of HSO_3Cl p.a. (Kemika) to $LiAlCl_4/SOCl_2$ led to the formation of $LiAl(SO_3Cl)_4$ salt [15,16]. Type D was catholyte C with the addition of chlorinated polymer (PVC, Solvic). Such a catholyte has not been used to date.

All salts were carefully dried before use. The content of water reaction products in electrolytes was controlled by i.r. spectroscopy (to be below 20 p.p.m.), the content of iron and sodium was controlled by atomic absorption spectroscopy (AA).

The cans of test cells were made of stainless steel. The surface area of the lithium electrodes (Foot Mineral) used was 9 cm^2. Two types of cathodes were used: (a) Knapsack acetylene black (Hoechst), 7% Teflon binder, further designated as type CL, and (b) 70% Knapsack acetylene black, 30% Ketjen black (Akzo Chemie), 7% Teflon binder, further designated as type MIL.

Lithium passive layer samples for morphology, thickness and composition determinations were prepared in an argon filled glove box with the relative humidity below 30 p.p.m. Scanning electron microscopy/energy dispersive spectroscopy (SEM/EDS) were made using a Jeol 220 microscope and Tracor X-ray analyser. The samples were transferred from the glove box into the microscope using a home-made vacuum-keeping device. Atomic absorption analyses (AA) were made on an ICP ARL-3520 spectrometer. All impedance, galvanostatic (delay effect) and capacity measurements were carried out on low current LT25 $Li/SOCl_2$ batteries at 20 °C and −25 °C. Before the measurements, one set of the batteries had been stored at room temperature for a period of six months and the other set for a period of 15 months. A Solartron 1250 frequency analyser and a 1286 electrochemical interface were used for the a.c. impedance measurements. The impedance spectra covered the frequency range of 0.1 Hz to 65 kHz. The Solartron 1286 electrochemical interface was also used for the galvanostatic (delay effect) measurements. Capacity (Ah) was measured at a constant load of 685 Ω (a current of ~ 5 mA) and at 3.3 kΩ (~ 1 mA).

3. Results and discussion

3.1 *SEM/EDS and impedance measurements*

It is known that lithium is passivated with a polycrystalline LiCl layer within approximately 100 s after

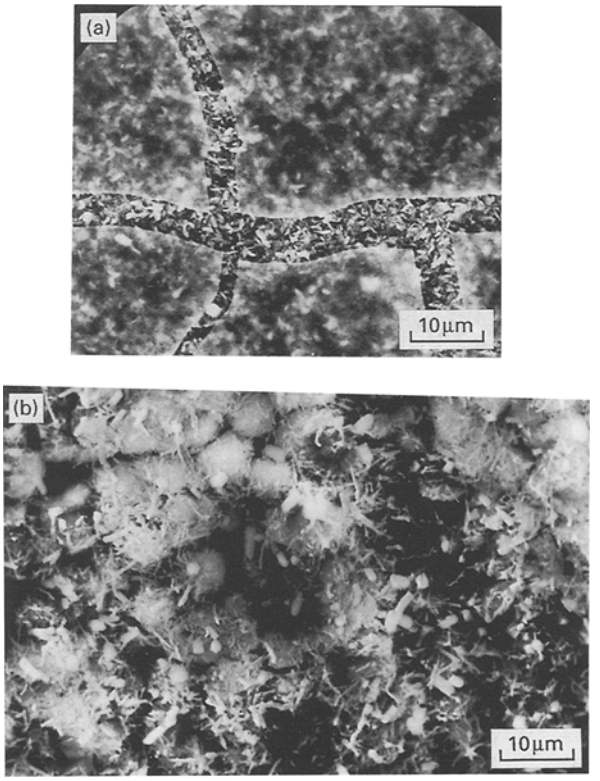

Fig. 2. Needle-like crystals were observed amongst which cubic ones could also be found in the electrolytes B (a) and D (b). PVC, dissolved in the electrolytes B and D, covered the surface of the passive layer.

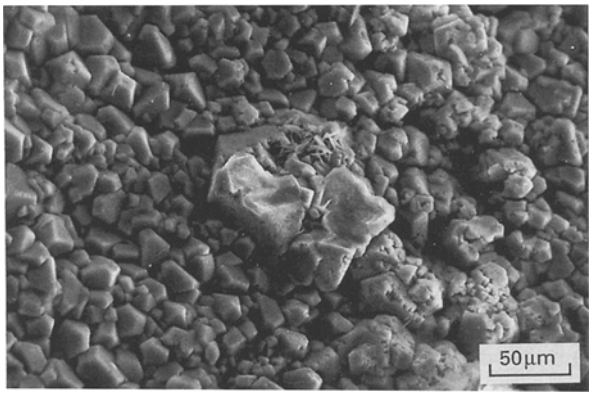

Fig. 3. SEM micrograph of lithium electrode surface after 12 days of exposure to electrolyte D. The LiCl morphology changed drastically; needle-like crystals were transformed into octahedrons or crystals of irregular shape.

exposure to a $SOCl_2$ electrolyte [2,17]. In the present study, the growth of LiCl on Li in electrolytes A, B, C and D was monitored by SEM/EDS and AA after 1 h, 7 day, 12 day and 15 month. In all the electrolytes passive layers were composed of LiCl with inclusions of Al^{3+} ions [6].

After 1 h, small crystals of LiCl were observed on the lithium surface. There was no difference in morphology of the crystals formed in different electrolytes but there was a difference in their abundance. The passivation was pronounced at places where mechanical and other defects on the lithium were observed. PVC, which was dissolved in the electrolytes B and D, also covered the surface of lithium and the passive layer.

After seven days of exposure of lithium to the electrolytes, some changes in morphology and in the dimensions of the LiCl crystals could be observed. In electrolyte A, cubic LiCl crystals were formed [1,2,6] whereas in the electrolyte C they had octahedral shape [6,8]. In electrolytes B and D (PVC additives), needle-like crystals were observed amongst which also cubic ones could be found (Fig. 2(a) and (b)). Average passive layer thicknesses that could be estimated from fractures formed during the preparation of passivated lithium for the SEM investigation, had values from 1 to 3 μm.

After 12 days, the LiCl crystals were bigger but their morphology remained the same as after seven days [6] except in the electrolyte D where the LiCl morphology changed drastically (Fig. 3). The needle-like crystals were transformed into octahedrons and/or into crystals of irregular shape. Apart from the SEM micrographs, the passive layer thicknesses were also calculated from AA data [6]; they were found to be of the same order of magnitude (3–15 μm).

After 15 months, the thickness and the morphology of the passive layers in the batteries at 20 °C remained constant, 3–20 μm, (Fig. 4(a) and (b)).

Some LiCl crystals were interlocked with separator fibres, as already found by Mogensen [2].

Using electron microscopy (SEM), geometric properties, e.g. the polycrystallinity and the approximate thickness of the passive layer, are relatively easy to estimate. It is instructive to compare these results with the impedance measurements when possible. If presented in the complex plane the measured frequency responses of all systems studied consist of two arcs, the high frequency (65 000 to about 1 Hz) and the low frequency (below 1 Hz). In the field of lithium batteries different semicircles are ascribed to different sublayers of the passive layer. This, however, often leads to atomic or subatomic thicknesses. Therefore, it can be suggested that the high capacity associated with the low-frequency arc indicates that a chemical (diffusion, adsorption) rather than the electrostatic storage of energy is involved. Consequently, we decided to compare with the SEM analysis only the resistance R_i and the capacitance C_i associated with the high frequency arc. The value of R_i increased with storage time in all the systems investigated. However, its values as well as the rate of its increase, markedly depended on both the electrolyte, and the cathode additives. The capacitance, C_i, decreased slightly with storage time and also depended on the type of additives used. Comparison between the passive layer thickness obtained by SEM and R_i against time curves reveals interesting results. For example, the resistances after 15 months of storage were in some cases two orders of magnitude higher than those after 12 days of storage, while the corresponding layer thicknesses remained within the same order of magnitude. Furthermore, the lowest thicknesses (2–10 μm) were observed with electrolytes A and B, i.e. in cases with the largest resistances and having

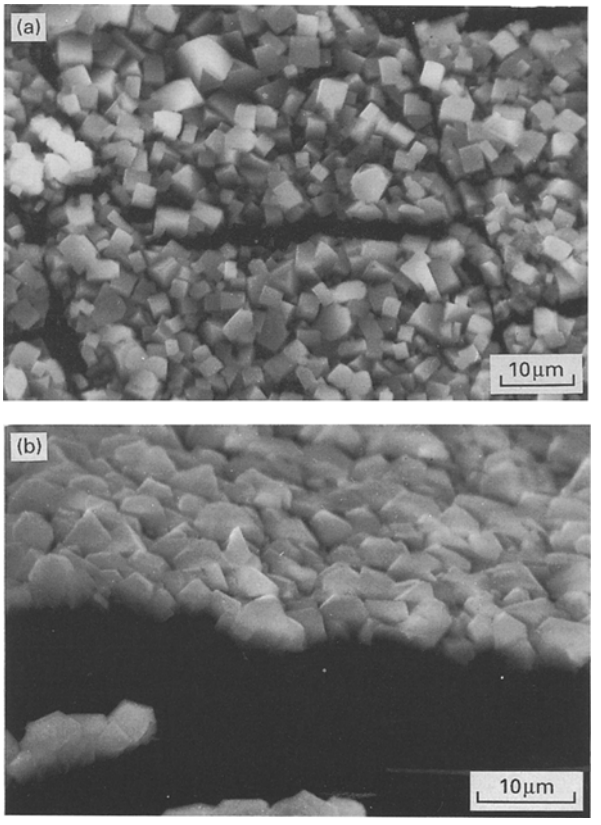

Fig. 4. SEM micrographs of the SEI on lithium electrode after 15 months of exposure to electrolytes A (a) and C (b). The morphology and dimensions of LiCl crystals is of the same order of magnitude as after 12 days.

Table 1. Average values of R_i and C_i found by fitting the high-frequency arc with Cole–Cole equation [20]. The classical (CL) type of cathode was used

(a) Batteries aged for six months

E	T/°C	R_i/Ω	C_i/F × 10^{-6}
A	20	1783	1.91
B	20	1217	2.57
C	20	541	1.22
D	20	150	1.48
A	−25	33 000	1.33
B	−25	41 000	1.81
C	−25	830	1.52
D	−25	355	4.57

(b) Batteries aged for 15 months

E	T/°C	R_i/Ω	C_i/F × 10^{-6}
A	20	1240	2.65
B	20	5470	1.53
C	20	508	1.08
D	20	193	1.35
A	−25	33 280	1.33
B	−25	70 000	1.39
C	−25	1408	1.68
D	−25	1168	2.57

E type of electrolyte
T temperature/°C
R_i interfacial resistance/Ω
C_i space charge capacitance/farads.

the most pronounced delay effect (Table 1, 2, Fig. 5 (a) and (b)). Both results directly show that the resistance of the passive layer is generally not related to its thickness. This is not in contradiction with the space charge model which regards both quantities as independent by definition. The thicknesses calculated from the measured capacitances represent a small percentage of the total thickness of the passive layer. The classical SEI approach ascribes this to the passive layer porosity that dominates over more than 90% of the passive volume. However, with SEM, pores extending from the electrolyte deep into the passive layer, as assumed by the classical SEI model, were not observed. Similarly, a two-layered microstructure of the passive layer corresponding to the primary (compact) and the secondary (porous) sublayer, as predicted by the classical SEI model, were also not observed. The two-layer structure should have been observed at least in batteries containing the MIL type of cathodes; there the thickness of the primary sublayer, calculated from the impedance response according to the classical SEI model, has a value of 0.1–0.25 μm so that it should be observable by SEM. Thus, as regards the microstructural properties of the passive layer the present results may be compared to those of Boyd [1] but do not support the classical SEI model. In all cases the relaxation time of the high frequency arc was time dependent. This cannot be explained by strictly referring to the classical SEI model which predicts a thickness and, thus, time-independent relaxation time.

Table 2. Average values of R_i and C_i found by fitting the high-frequency arc with Cole–Cole equation [20]. The MIL type of cathode was used

(a) Batteries aged for six months

E	T/°C	R_i/Ω	C_i/F × 10^{-6}
A	20	212	0.466
B	20	218	0.539
C	20	46	1.19
D	20	36	0.577
A	−25	1154	2.53
B	−25	4637	1.64
C	−25	1000	8.99
D	−25	598	16.3

(b) Batteries aged for 15 months

E	T/°C	R_i/Ω	C_i/F × 10^{-6}
A	20	422	0.256
B	20	379	0.414
C	20	171	0.241
D	20	135	0.462
A	−25	5200	1.75
B	−25	3912	2.71
C	−25	1171	6.52
D	−25	802	7.23

E type of electrolyte
T temperature/°C
R_i interfacial resistance/Ω
C_i space charge capacitance/farads.

3.2. *Galvanostatic measurements*

Galvanostatic measurements were carried out at relatively high currents (10 mA, 5 mA) and in the nonlinear regime, in contrast to the impedance measurements that were performed in the linear regime. In the case of lithium batteries nonlinear measurements have been much more common than linear ones. It is easy to show that the nonlinear regime (above 10 mV) may begin at current densities as low as 0.1–0.25 μA cm^{-2}. However, the batteries are expected to operate, and are consequently tested, at much higher current densities. The fact that the tests are almost regularly performed in the nonlinear regime may, to some extent, explain their low reproducibility.

It has been reported [19] that generally there is no direct relationship between the impedance spectroscopy and the galvanostatic or potentiostatic discharge measurements (delay effect measurements) because the latter method is regularly applied deeply in the nonlinear region. Nevertheless, many experiments have shown that the following empirical rule may frequently be used: the higher the resistance of the high-frequency arc the larger is the initial voltage (or current) drop in galvanostatic or potentiostatic measurements (at time resolution of about 1 s). The rule is valid for batteries with the same type of electrolyte, and in cases when large variation of resistance is involved. Thus, the impedance method may be used as a non-destructive method for a rough estimation of the initial voltage drop during the delay effect measurements. Comparing Figs. 5(a), (b), 6(a), (b), and Table 3 it can be seen that the rule is reasonably

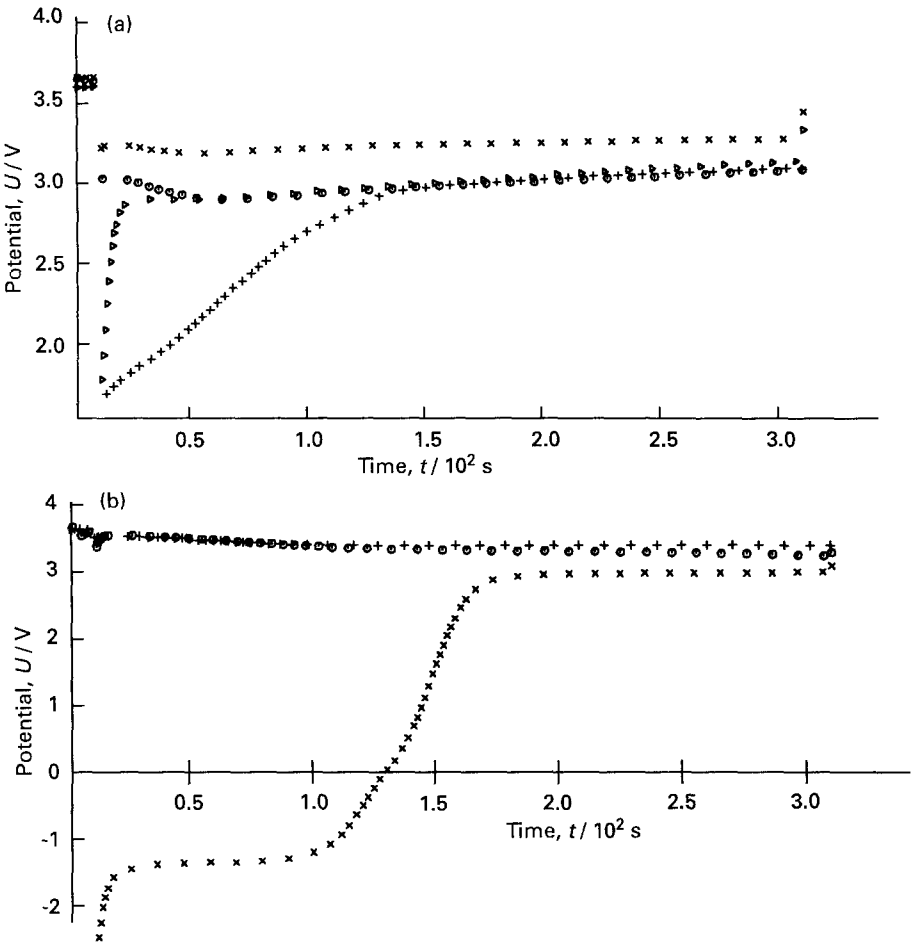

Fig. 5. Delay effect for six month old batteries. (a) Electrolytes A (△), B (+), C (⊙) and D (×) and CL type of cathode; discharge current density was 10 mA, time of discharge 300 s, temperature 20 °C. (b) Electrolytes A (×), C (⊙) and D (+) and CL type of cathode; discharge current density was 10 mA, time of discharge 300 s, temperature −25 °C.

well obeyed. The smallest initial voltage drop was observed with electrolytes C and D, and the largest with A and B. The shape of the time–voltage curve at times above 1 s should be related to the low-frequency arc impedance response. However, due to the non-linearity, the shape of the galvanostatic curve cannot be predicted from the linear impedance measurements.

The best time–voltage results for galvanostatic discharge measurements were found for the electrolyte D, which showed practically no delay effect at current densities of up to 1.13 mA cm^{-2}.

3.3. *Space charge model*

It has been shown (cf. 11–13) that the electrochemical behaviour of Li/$SOCl_2$ systems may be compared to the behaviour of a Schottky diode. This means that the transport in this system is not controlled by migration through the bulk of the passive layer (classical SEI model) but by the space charge region at the Li/passive layer phase boundary. This region contributes essentially to the total interfacial resistance and determines the capacitance.

The space charge region is formed during the passive layer growth. Its final shape may be reached as late as after several days or even weeks after immersion of lithium in $SOCl_2$ solution. This means that during that time the resistance, the capacitance and also their product RC (the relaxation time) are being changed, which has been observed in all systems studied. Also the delay effect of Li/$SOCl_2$ batteries may be explained by referring to the space charge model. Similarly as with a Schottky diode, the thickness of the space charge region depends on the magnitude and sign of the external bias (overpotential). In the anodic direction, the shape of the space charge region approaches to the flat band situation, which means that the average concentration of charge carriers in that region grows with the increasing anodic bias. However, unlike the Schottky diode, the time needed to change the space charge shape is very long, tens of seconds or even more. During that time the resistance of the interfacial region gradually drops, causing the so called delay effect of lithium batteries (Fig. 7). The much slower response of the space charge in the passive layer if compared to the response of the Schottky diode, may be ascribed to the fact that in the former case the charge carriers with low mobility are ions, while in the latter the carriers with high mobility are electrons. The effect of additives on the resistance, capacitance and the delay effect may also be explained using the space charge model. Although the precise mechanism of the influence of additives on the electrical properties of the

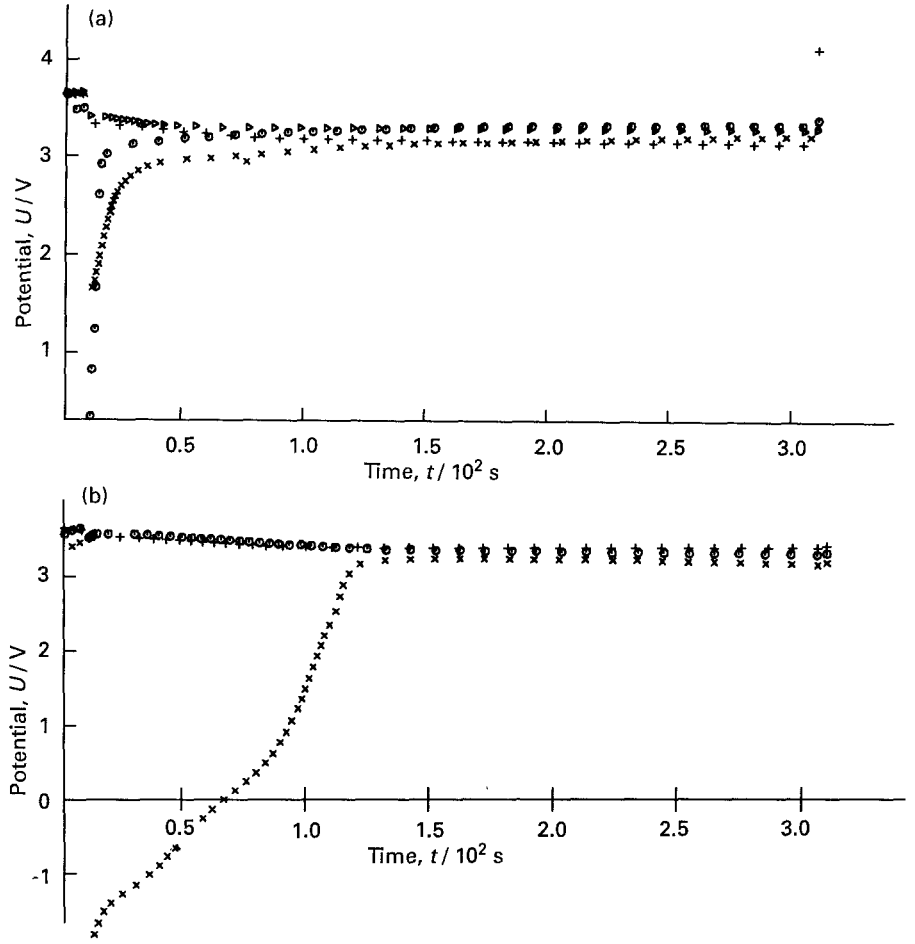

Fig. 6. Delay effect for 15 month old batteries. (a) Electrolytes A (×), B (⊙), C (+) and D (△) and CL type of cathode; discharge current density was 10 mA, time of discharge 300 s, temperature 20 °C. (b) Electrolytes A (×), C (⊙) and D (+) and CL type of cathode; discharge current density was 10 mA, time of discharge 300 s, temperature −25 °C.

passive layer is not known, two or three effects are probable: the additives control the polycrystallinity and the degree of doping of the passive layer with aluminium. If one or both properties are enhanced, the average bulk, and hence also the space charge concentration of mobile charge carriers, is increased, which leads to a decrease of the bulk and the space charge resistance. Also plausible is the explanation that the additives modify the microstructure of the Li/passive layer interface, by which the barrier for the electrochemical reaction and the shape of the space charge region is changed. We have not been able to find an approximate rule for comparing the results of both techniques. This renders the explanation for different time–voltage behaviour of passive layers grown in various electrolytes difficult. According to the space charge model it may be assumed that the time necessary to reach the steady voltage response depends on the mobility of the less mobile species, the higher the mobility the shorter the time. As mobility strongly depends on temperature, the delay effect is much more pronounced at low temperatures (−25 °C) than at high ones (e.g. +20 °C), (Fig. 5(a) and (b)).

Table 3. R_i, U_{min} and $U_{ocv} - U_{min}$ values for six month old batteries with different types of electrolytes and two different types of cathodes

E	T/°C	R_i/Ω	I/mA	U_{min}/V	$U_{ocv} - U_{min}$/mV
A CL	20	1793	10	1.458	2212
B CL	20	1268	10	1.584	2086
C CL	20	266	10	2.836	834
D CL	20	150	10	3.165	505
A MIL	20	234	10	2.859	791
B MIL	20	235	10	1.619	2031
C MIL	20	62	10	2.836	814
D MIL	20	35	10	3.342	310
A CL	−25	32000	10	−2.67	6340
C CL	−25	1004	10	3.160	510
D CL	−25	398	10	3.377	293
A MIL	−25	1220	5	2.958	692
B MIL	−25	4364	5	3.180	470
C MIL	−25	1029	5	3.137	513
D MIL	−25	598	5	3.102	548

E different types of electrolytes and cathodes
U_{min} minimum voltage value (V) during discharge
$U_{ocv} - U_{min}$ voltage difference between open circuit voltage (ocv = 3.68 V) and U_{min} (mV)
I discharge current (mA).

3.4. *Capacity measurements*

The average capacity of a battery after six and 15 months shelf-life may be used as a measure of lithium corrosion in that battery. While the battery discharge behaviour is governed by the ionic conductivity, the

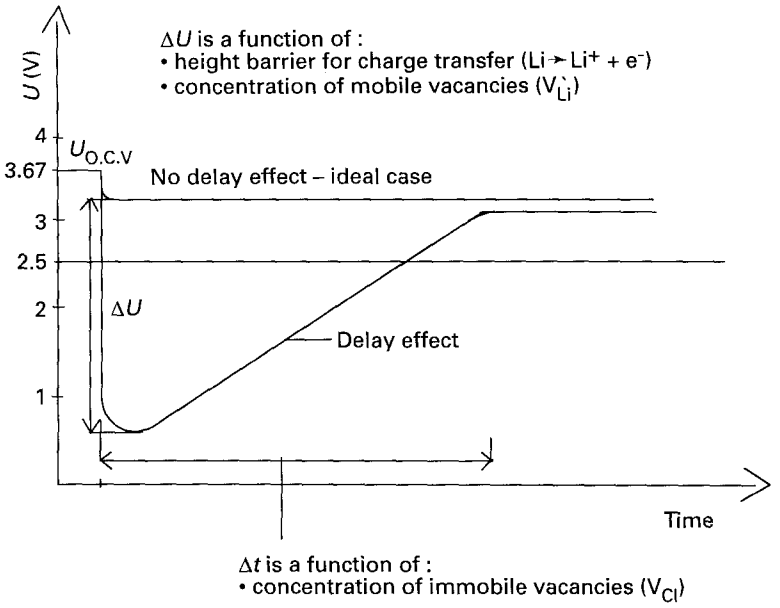

Fig. 7. Delay effect as a consequence of the different barrier for electrochemical reaction ($Li \rightarrow Li^{+} + e^{-}$), different mobility and concentration of the charge carriers; in our case the more mobile are V_{Li}, vacancies and the less mobile are V_{Cl} vacancies.

lithium corrosion during the battery shelf-life is dominated by the electron conductivity. The ionic conductivity is approximately determined by R_i, i.e. the charge transfer resistance on the Li/LiCl interface, whereas the resistance of the ionic transport through the bulk is negligible. As regards the electron transport, it is not known whether the interface or the bulk resistance is prevailing. If the interfacial resistance prevails, R_i and the lithium corrosion are connected. This possibility, however, cannot be verified by the inspection of results summarized in Tables 1 and 2 and 4(a) and (b). It can be assumed that, not only the interface conductivity, but also electron transport through the bulk contributes to lithium corrosion.

Theoretically, lithium in the batteries provides 2.06 Ah. The additives in electrolytes B, C and D had no influence on lithium corrosion, cf. Table 4(a). The highest capacities were obtained with electrolyte D at −25 °C. Comparing the reference batteries using electrolyte A, lower capacities were obtained when electrolytes C and D were used together with MIL cathodes. The combination of additives enhanced the corrosion by 8% after six months, cf. Table 4(b). Experimental results also showed that MIL type cathodes are suitable only for low discharge current batteries of a maximum of 1 mA.

Table 4. Battery capacities for electrolytes A, B, C and D

(a) *Cathode type CL*
Batteries were discharged at loads 685 Ω (discharge current was approximately 5 mA).

	6 months old		*15 months old*	
E	*T*/20 °C	*T*/−25 °C	*T*/20 °C	*T*/−25 °C
A	92.2%	61.6%	70.1%	58.0%
B	90.8%	58.7%	72.1%	43.7%
C	96.1%	53.3%	70.1%	49.6%
D	89.8%	75.5%	92.7%	76.7%

(b) *Cathode type MIL*
Batteries were discharged at loads 3.3 kΩ (discharge current was approximately 1 mA

	6 months old	
E	*T*/20 °C	*T*/−25 °C
A MIL	92.2%	79.1%
B MIL	91.7%	97.0%
C MIL	80.6%	58.7%
D MIL	84.0%	64.1%

Q capacities/%
T discharge temperature/°C.

4. Conclusions

In summary:

(i) Electrical and microstructural properties of the passive layers formed on lithium in $SOCl_2$, containing different additives (PVC, inorganic salts, cathode additives), were studied. It was found that in all cases the morphology and the resistance of the passive layer strongly depended on storage time, while the capacity and the thickness of the passive layer varied much less with time.

(ii) LiCl crystals were cubic (electrolyte A), octahedral (electrolyte B) or needle-like (PVC containing additives). Typical passive layer thicknesses were 1–20 μm. Neither porosity nor a two-layer structure of the passive layer was observed.

(iii) The electrical properties of the passive layer were explained by the space charge model of SEI conduction rather than the classical SEI model. Thus, the high-frequency arc was ascribed to the conduction across the Li/passive layer interface rather than to the bulk conduction of the passive layer.

(iv) Impedance spectroscopy may be selectively used as a non-destructive method for estimation of the galvanostatic behaviour of lithium batteries.

(v) The delay effect was most successfully eliminated with a combination of organic and inorganic additives in electrolyte (electrolyte D). These additives did not reduce the battery capacity. However, if additives were also used in cathodes (MIL type cathodes) the battery capacity was decreased by 8% after storage for six months.

References

[1] J. W. Boyd, *J. Electrochem. Soc.* **134** (1987) 18.
[2] M. Mogensen, Riso National Laboratory, DK-4000 Roskilde, Denmark (1987).
[3] M. Gaberšček, J. Jamnik and S. Pejovnik, *J. Power Sources* **25** (1989) 123.
[4] S. Dallek, S. D. James, W. P. Kilroy, *J. Electrochem. Soc.* **128** (1981) 508.
[5] R. V. Moshtev, Y. Geronov and B. Puresheva, *ibid.* **128** (1981) 1851.
[6] M. Kovač, M. Jakič and S. Pejovnik, Sixth International Meeting on Lithium Batteries, Munster, Germany (1992) p. 495.
[7] M. Jakič, M. Kovač and S. Pejovnik, Sixth International Meeting on Lithium Batteries, Munster, Germany (1992) p. 498.
[8] P. Chenebault, D. Vallin, J. Thevenin and R. Wiart, *J. Appl. Electrochem.* **18** (1988) 625.
[9] P. Chenebault, D. Vallin, J. Thevenin and R. Wiart, *ibid.* **19** (1989) 413.
[10] E. Peled, *in* 'Lithium Batteries' (edited by J. P. Gabano), Academic Press, New York (1983) chapter 3.
[11] J. Jamnik, M. Gaberšček, A. Meden and S. Pejovnik, *J.Electrochem. Soc.* **138** (1991) 1582.
[12] M. Gaberšček, J. Jamnik and S. Pejovnik, *ibid.* **140** (1993) 308–314.
[13] M. Gaberšček, J. Jamnik and S. Pejovnik, Sixth International Meeting on Lithium Batteries, Munster, Germany (1992) p. 203.
[14] Y. Haven, *Recueil* **69** (1950) 1471.
[15] D. Vallin, P. Chenebault, Proc. 32nd Power Sources Symposium, The Electrochemical Society, Penington, NJ (1986) p. 481.
[16] W. J. Bowden, J. S. Miller, D. Cubbison and A. N. Dey, *J. Electrochem. Soc.* **131** (1984) 1768.
[17] W. M. Hedges, D. Pletcher and C. Gosden, *ibid.* **134** (1987) 1334.
[18] I. D. Raistrick, *in* 'Impedance Spectroscopy', (edited by J. R. Macdonald), John Wiley & Sons, New York (1987) p. 67.
[19] J. Jamnik, M. Gaberšček and S. Pejovnik, Sixth International Meeting on Lithium Batteries, Munster, Germany (1992) p. 470.
[20] K. S. Cole and R. H. Cole, *J. Chem. Phys.* **9** (1941) 341.
[21] C. R. Schlaikjer and C. Young, Power Sources Symposium (1980) p. 129.
[22] T. Osaki, *J. Power Sources* **20** (1987) 61.